Applied Catalysis B: Environmental 84 (2008) 393–399

Contents lists available at ScienceDirect

Applied Catalysis B: Environmental

journal homepage: www.elsevier.com/locate/apcatb

Mineralization of an azo dye Acid Red 14 by photoelectro-Fenton process using an activated carbon fiber cathode

Aimin Wang, Jiuhui Qu *, Huijuan Liu, Jia Ru

State Key Laboratory of Environmental Aquatic Chemistry, Research Center for Eco-Environmental Sciences, Chinese Academy of Sciences, Beijing 100085, China

ARTICLE INFO

Article history:
Received 1 March 2008
Received in revised form 13 April 2008
Accepted 16 April 2008
Available online 22 April 2008

Keywords:
Photoelectro-Fenton process
Mineralization
Acid Red 14
Activated carbon fiber cathode

ABSTRACT

The mineralization of an azo dye Acid Red 14 (AR14) by the photoelectro-Fenton (PEF) process was studied in an undivided electrochemical reactor with a RuO_2/Ti anode and an activated carbon fiber (ACF) cathode able to electrochemically generate H_2O_2. Anodic oxidation and UV irradiation of AR14 were also examined as comparative experiments. Results indicate that the electro-Fenton process yielded about 60–70% mineralization of AR14, while the photoelectro-Fenton could mineralize AR14 more effectively (more than 94% total organic carbon (TOC) removal) even at low current densities assisted with UV irradiation after 6 h electrolysis. The mineralization current efficiency (MCE) of the PEF process increased with the increasing AR14 concentrations. In addition, the initial solution pH ranging from 1.49 to 6.72 had little influence on the TOC removal probably due to the formation of organic carboxylic acids which balanced the pH increase caused by the cathodic generation of hydrogen gas. The ACF cathode showed a long-term stability during multiple experimental runs for degradation of AR14, indicating its good potential for practical application in treating refractory organic pollutants in aqueous solutions.

1. Introduction

Dyes present in wastewater are of particular environmental concern since they not only give an undesirable color to the waters but also in some cases are themselves harmful compounds and can originate dangerous byproducts through oxidation, hydrolysis, or other chemical reactions taking place in the waste phase [1]. Most dyes are toxic and recalcitrant to biodegradation, causing a decay in the efficiency of biological plants currently used for the treatment of such wastewaters [2]. To avoid the dangerous accumulation of dyes in the environment, there is a need to develop effective methods for the degradation of such organic pollutants, either to less harmful compounds or, more desirable, to their complete mineralization.

Various treatment processes have been investigated to reduce dye concentrations in water and to minimize the potential health risks associated with exposure to the chemicals through consumption of contaminated waters. In recent years indirect electrooxidation methods with hydrogen peroxide electrogeneration, such as electro-Fenton (EF) and photoelectro-Fenton (PEF) reactions, are being developed for the treatment of toxic and refractory organic pollutants in acid waters [3–30]. In these environmentally friendly electrochemical techniques, hydrogen peroxide is continuously generated in an acidic contaminated solution from the two-electron reduction of O_2 which takes place on graphite [3–5], reticulated vitreous carbon [6–9], mercury pool [10–12], carbon-felt [13–18] O_2-diffusion [19–29] and activated carbon fiber (ACF) [30] cathodes. In acidic aqueous medium the oxidation power will be enhanced by addition of ferrous ions to the solution that allows the production of a very reactive one-electron oxidizing agent hydroxyl radical ($^{\bullet}OH$) (E° = 2.8 V/NHE) from the well-known Fenton reaction between both species with a second-order rate constant k_2 = 53 M^{-1} s^{-1} [11]. This $^{\bullet}OH$ radical acts as a non-selective, very strong oxidant agent with ability to react with organics giving dehydrogenated or hydroxylated derivatives, until achieving their total mineralization, i.e., their conversion into CO_2, water and inorganic ions [19]. The electro-Fenton process can generate $^{\bullet}OH$ by the simultaneous electrochemical reduction of O_2 in the presence of catalytic amounts of ferrous ions [14]:

$$O_2 + 2H^+ + 2e^- \rightarrow H_2O_2, \quad E^{\circ} = 0.69\,\text{V/NHE} \tag{1}$$

$$Fe^{2+} + H_2O_2 + H^+ \rightarrow Fe^{3+} + H_2O + {}^{\bullet}OH, \quad k = 63\,\text{L mol}^{-1}\,\text{s}^{-1} \tag{2}$$

$$Fe^{3+} + e^- \leftrightarrow Fe^{2+}, \quad E^{\circ} = 0.77\,\text{V/NHE} \tag{3}$$

$$H_2O \leftrightarrow \frac{1}{2}O_2 + 2H^+ + 2e^-, \quad E^{\circ} = 1.23\,\text{V/NHE}$$

However, a significant drawback is the parasitic reactions, e.g., electrolysis of water often compete with the O_2 reduction and

* Corresponding author. Tel.: +86 10 62849151; fax: +86 10 62923558.
E-mail addresses: jhqu@rcees.ac.cn, hjliu@rcees.ac.cn (J. Qu).

0926-3373/$ – see front matter © 2008 Elsevier B.V. All rights reserved.
doi:10.1016/j.apcatb.2008.04.016

lower the energy efficiency [31]. Moreover, under most conditions pollutant impurities are present at such low concentrations that electrochemical processes are diffusion-controlled. The resulting diffusion-limited currents can, however, be enhanced at high-area, porous electrodes at which 2-dimensional electrochemistry is converted to "quasi-3-dimensional" behavior due to the large distributed area [32]. In our laboratory, the large surface area of ACF felt (BET 1297 $m^2\,g^{-1}$) was developed for the cathode of electro-Fenton reaction. The mineralization of azo dye Acid Red 14 (AR14) by electro-Fenton reaction was achieved efficiently using the ACF felt cathode, at pH 3.0 and applied current 0.36 A, after 360 min electrolysis the total organic carbon (TOC) removal rate for 500 mL of a 200 mg L^{-1} AR14 in solution was 70% [30].

The oxidation power can be enhanced by introduced UV light into electro-Fenton process. UV light can accelerate the mineralization process by: (i) the photodecomposition of complexes of Fe^{3+} with generated carboxylic acids, e.g., oxalic acid. That is, at acidic pH, oxalic acids behave as photo-active complexes in the presence of ferric ions which undergo photo-decarboxylation reaction [33]:

$$Fe(III)(RCO_2)^{2+} + h\nu \rightarrow Fe^{2+} + CO_2 + R^{\bullet} \quad (5)$$

and (ii) the regeneration of more Fe^{2+} from the additional photoreduction of $Fe(OH)^{2+}$, which is the predominant Fe^{3+} species in acid medium [20]:

$$Fe(OH)^{2+} + h\nu \rightarrow Fe^{2+} + {}^{\bullet}OH \quad (6)$$

The objective of this work is to investigate the photoelectro-Fenton process based on ACF felt cathode for degradation of AR14 so as to compare the oxidative capability with electro-Fenton process. We focused on systematically investigating the degradation of AR14, a model chemical throughout the study to represent toxic contaminants with aromatic structures, by photoelectro-Fenton process. The effect of UV light, pH, Fe^{2+} concentration, initial AR14 concentration, iron ion type and applied current were also studied in detail in the experimental runs.

2. Experimental

2.1. Materials

The activated carbon fiber felt was obtained from Xuesheng Technology Co. Ltd. (Shandong, China), and its BET surface area, total pore volume, and mean micropore size of ACF, measured from N_2 adsorption using Micromeritics Model ASAP 2000, were shown in our another paper [30].

Acid Red 14(AR14), a commercial azo dye, whose chemical structure was given in Fig. 1, was used without further purification. Sulfuric acid, anhydrous sodium sulfate and heptahydrated ferrous sulfate were of analytical grade. Deionized and double distilled water was used throughout this study.

2.2. Electrolytic system

The experiments were conducted in an open, undivided cell with a capacity of about 0.5 dm^3 including an 11 W low pressure mercury lamp was positioned in a hollow cylindrical quartz tube (Fig. 2). The experiments were performed at constant currents supplied by a DC power supply. The 20 cm^2 (4 cm × 5 cm) area ACF felt was selected as cathode. A titanium grid, on the ACF felt, ensured the electric contact. The same solid surface area RuO_2/Ti mesh was selected as anode. The electrode distance was 4.5 cm. The solution was continuously stirred with a magnetic bar.

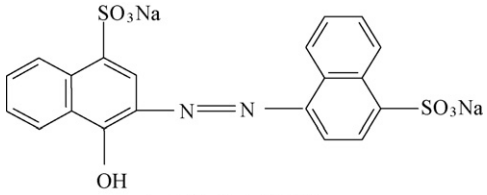

Acid Red 14 (AR14)
C. I. 14720

Fig. 1. Chemical structure for Acid Red 14 (AR14).

Prior to each electrolysis, the ACF felt cathode was first presaturated with 400 mg L^{-1} AR14 solution for 12 h to preclude the TOC decrease due to AR14 adsorption on ACF felt. AR14 was comparatively degraded in an acidic aqueous medium containing 0.05 M Na_2SO_4 as supporting electrolyte and 0.2 M H_2SO_4 was added to adjust its initial pH to 3.0 using an Orion model 720APLUS Benchtop pH meter (Thermo Orion Co., USA). Solutions of 450 mL with 200 mg L^{-1} of initial AR14 concentration were electrolyzed at constant current. During the electrolysis, O_2 was sparged near the cathode surface to ensure the essential oxygen for electrochemical reactions. A catalytic quantity of ferrous ion was introduced into the solution before the beginning of electrolysis.

2.3. Analytical method

Samples were withdrawn from the reactor at regular time intervals (0, 30, 60, 120, 180, 270, and 360 min, etc.). UV–vis spectra of the samples were recorded, between 190 and 650 nm, on a U-3010 UV–vis spectrophotometer (Hitachi Co., Japan) equipped with 10 mm quartz cuvettes. The decolorization of the solution was achieved by measuring the absorbance of the diluted samples (typically 1:4 in water) at 514 nm. The total organic carbon of the initial and electrolyzed samples was determined with Phoenix 8000 TOC analyzer (Tekmar–Dohrmann Co., USA).

The mineralization current efficiency (MCE) at a given time for the above solutions was then comparatively estimated from the following equation [23]:

$$MCE = \frac{\Delta(TOC)_{exp}}{\Delta(TOC)_{theo}} \times 100 \quad (7)$$

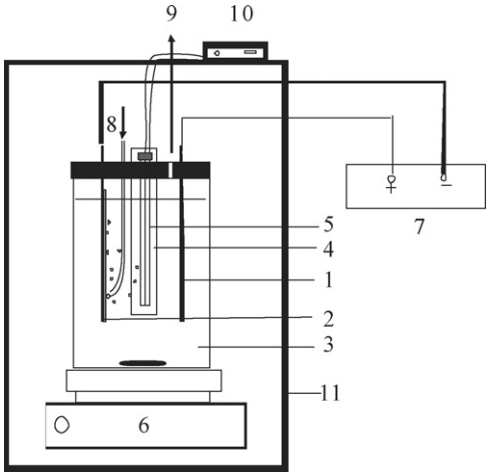

Fig. 2. Experimental set-up of the photoelectro-Fenton reactor. (1) RuO_2/Ti anode; (2) ACF cathode; (3) AR14 solution; (4) quartz tube; (5)11 W low-pressure Hg lamp; (6) magnetic stirrer; (7) DC supply; (8) O_2 in; (9) sampling; (10) UV switch; and (11) dark box.

where $\Delta(TOC)_{exp}$ is the experimental TOC decay ($[TOC]_0-[TOC]_t$) and $\Delta(TOC)_{theo}$ is the theoretically calculated TOC decay assuming that the applied electrical charge (=current × time) is only consumed in the mineralization process of AR14.

Hydrogen peroxide concentrations were determined spectrophotometrically by the iodide method with a UV–visible spectrophotometer (Hitachi 3010) at λ = 352 nm (ε = 26400 M^{-1} cm^{-1}) [34].

3. Results and discussion

3.1. Comparative degradation behavior

Fig. 3 summarized the results of TOC decay relative to AR14 degradation by: (a) ACF cathode adsorption; (b) UV irradiation; (c) RuO_2/Ti anodic oxidation; (d) electro-Fenton; (e) electrogenerated H_2O_2 under UV exposition, and (f) photoelectro-Fenton conditions, respectively. The applied current was constant at 0.36 A. As could be seen, the use of ACF felt adsorption alone on AR14 led to a limiting removal of about 11% after 360 min. Similarly anodic oxidation alone could only reduce TOC less than the 14%, and UV irradiation 15%. The low adsorption ability that was attributed to the ACF felt had been presaturated before every experiment. The low oxidative ability of anodic oxidation could be explained by the lower $^{\bullet}OH$ concentration formed on the RuO_2/Ti anode surface generated from water oxidation from reaction (8) [28], which was the main oxidizing agent of AR14 and its oxidation products in both cases. The decomposition rate of AR14 in electro-Fenton was enhanced using the ACF felt cathode since the TOC of solution was reduced by 59% after 360 min electrolysis. It could be ascribed to the existence of fast homogeneous reaction of organics with the great amounts of $^{\bullet}OH$ generated from reaction (2), which could oxidize nonselectively most products remaining in the solution. In contrast, a significant acceleration in the presence of UV, the electrogenerated H_2O_2 under UV exposition and the PEF method with 1 mM Fe^{2+} had the higher oxidative ability, since the TOC of solution was reduced by 91% and 95% after 360 min electrolysis for electrogenerated H_2O_2 under UV exposition and PEF process, respectively. The fast TOC removal in electrogenerated H_2O_2 under UV exposition process may contribute to the hydroxyl radicals generated by H_2O_2 photolysis, although the stable concentration of H_2O_2 considered in this process is only about 600 μM [30]. At 254 nm, H_2O_2 absorbs radiation with a molar absorption coefficient of 18.6 $L\,M^{-1}\,s^{-1}$, it decomposes with a quantum yield of 0.98, generating $^{\bullet}OH$ radical (Eq. (9)) [35]. At the same time, the total mineralization achieved in PEF process could be ascribed to not only hydroxyl radicals from H_2O_2 photolysis but also to the two processes: the fast photodecomposition of Fe^{3+}–oxalatto complexes by UV light and the additional photo-reduction of $Fe(OH)^{2+}$ species according to the reaction (6), which could supply additional Fe^{2+} and hydroxyl radicals for the mineralization of AR14.

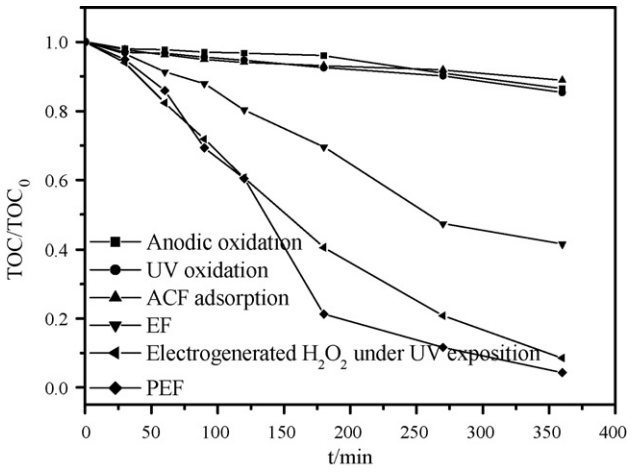

Fig. 3. TOC reduction as a function of treatment time for the ACF cathode adsorption, RuO_2/Ti anodic oxidation, UV irradiation, electro-Fenton, electrogenerated H_2O_2 under UV exposition and photoelectro-Fenton conditions.

$$H_2O \rightarrow {}^{\bullet}OH_{ads} + H^+ + e^- \quad (8)$$

$$H_2O_2 + h\nu \rightarrow 2{}^{\bullet}OH \quad (9)$$

3.2. Effect of UV light and current efficiency for the mineralization process

The effect of UV light to mineralize a 200 mg L^{-1} AR14 solution previously electrolyzed at 0.36 A during different times is depicted in Fig. 4a. The PEF degradation of 450 mL of a 200 mg L^{-1} AR14 solution was studied in a pilot reactor using an ACF cathode and a RuO_2/Ti anode. Fig. 4a shows the TOC removal for the AR14 solution at a regulated pH 3.0. When the solution was electrolyzed at 0.36 A in the EF process, a slow mineralization stage was reached after ca. 270 min with a TOC abatement of ca. 50%. This is due to the generation of quite stable intermediates such as oxalic acid. After 270 min electro-Fenton treatment, the solution was exposed to UV light and a fast TOC removal occurred to reach more than 99% mineralization in 90 min, and total mineralization was reached.

The above considerations allow the conclusion that mineralization of AR14 involves its conversion into CO_2, H_2O, NO_3^- and SO_4^{2-}. So the mineralization reaction can be written as follows [16,23]:

$$C_{20}H_{12}N_2S_2O_7Na_2 + 102\,{}^{\bullet}OH \rightarrow 20CO_2 + 2Na^+ + 2SO_4^{2-} + 2NO_3^- + 55H_2O + 4H^+ \quad (10)$$

which is equivalent to the electrochemical oxidation reaction

$$C_{20}H_{12}N_2S_2O_7Na_2 + 47H_2O \rightarrow 20CO_2 + 2Na^+ + 2SO_4^{2-} + 2NO_3^- + 106H^+ + 102e^- \quad (11)$$

where 102 electrons are involved in the destruction of each molecule of AR14.

The mineralization current efficiencies for the experiments given in Fig. 4a were then calculated from Eq. (7), considering reaction (11) to evaluate $\Delta(TOC)_{theo}$. The corresponding MCE-time plots thus obtained are presented in Fig. 4b. It can be found that the MCE of PEF process was much higher than that of EF process, it progressively rises during longer times at early stages of the treatment, reaching a maximum value of about 23% at 3 h. This suggests an increasing formation of products that react more easily with $^{\bullet}OH$ than the AR14 at early stages of electrolysis. After 3 h, the MCE decreases with electrolysis prolonged, which indicates that there are little organic products in the solution, $^{\bullet}OH$ cannot degrade them efficiently. It was also obvious from Fig. 4 that the UV light might enhance the MCE of EF process largely, when the UV light was turned on, the MCE increased rapidly.

3.3. UV–vis spectra changes in photoelectro-Fenton process

To clarify the changes of molecular and structural characteristics of AR14 as a result of electrolysis in the PEF process, representative UV–vis spectra changes of the dye solution as a function of electrolysis time were depicted in Fig. 5. As could be observed from these spectra, before the treatment, the absorption

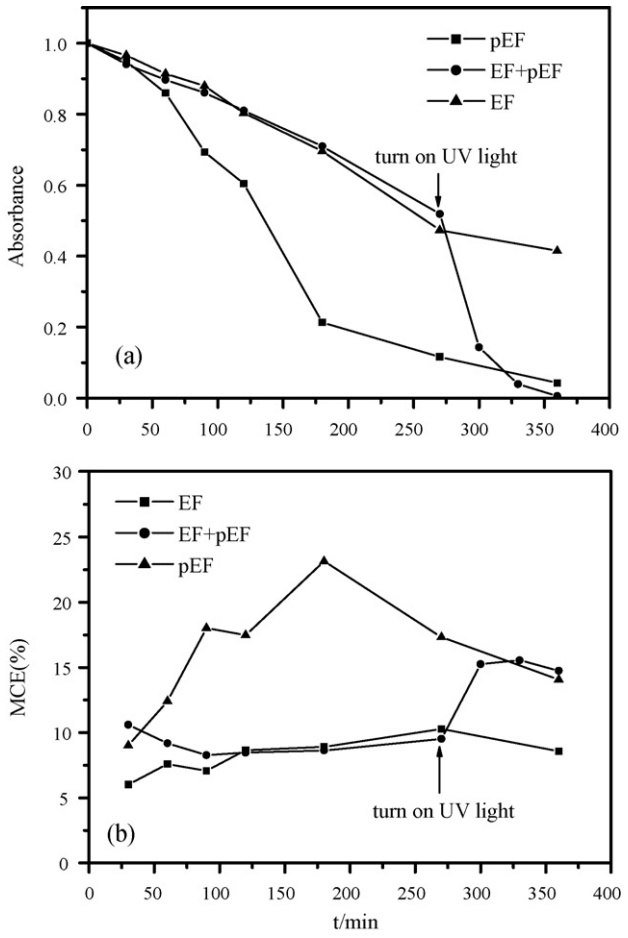

Fig. 4. Change of the mineralization current efficiency calculated from Eq. (8) with time for electro-Fenton and photoelectro-Fenton.

spectrum of AR14 in water was characterized by one main band in the visible region, with its maximum absorption at 514 nm, and by two bands in the ultraviolet region located at 220 nm and 322 nm. The peaks at 220 and 322 nm were ascribed to the absorption of the π–π^* transition related to the naphthalene rings bonded to the –N=N– group in the dye molecule [36,37]. The band in the visible region was attributed to the chromophore-containing azo linkage of the dye molecules in solution [38]. The adsorption peak at λ = 514 nm diminished and finally disappeared completely under 360 min electrolysis, indicating a rapid degradation of AR14. The intensity of absorption between 210 and 322 nm also rapidly decreased during the PEF treatment, which indicated the full destruction of the naphthalene rings. This is much obvious from comparing the Fig. 6a and b, which are the UV spectra change in the wavelength range of 190–265 nm for EF and PEF process, respectively. In PEF process, the UV absorption is removed more rapidly and completely than that in EF process, which indicates that the total mineralization was achieved in the PEF process. The transition of the UV–vis adsorption spectra of AR14 confirmed that photoelectro-Fenton method was an effective electrochemical treatment for degradation of refactory organic pollutant in water.

3.4. Effect of applied current

A series of electrolyses with ACF cathode were carried out with 200 mg L^{-1} of AR14 in the current density range 0–0.50 A. As shown in Fig. 7, it was found that increasing current density in the range 0–0.36 A causes quicker mineralization rate in the PEF process due to

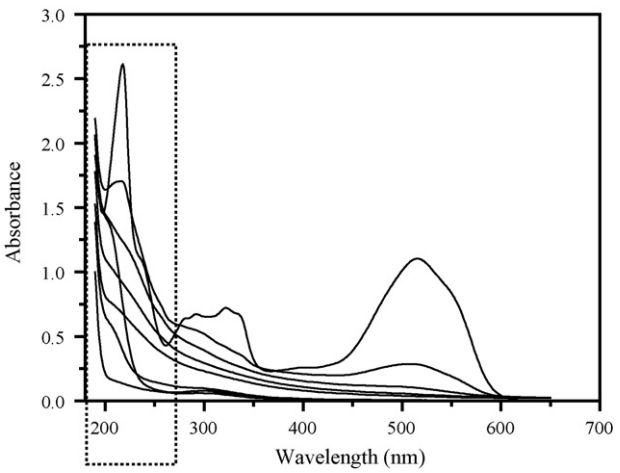

Fig. 5. UV/vis spectral changes with electrolysis time for 450 mL of 200 mg L^{-1} AR14 solution in 0.05 M Na_2SO_4 of pH 3.0. Experimental conditions: applied current = 0.36 A; $[Fe^{2+}]$ = 1 mM, (samples were diluted for 5 folds before monitoring).

the concomitant production of more •OH in the medium from reaction (2) and (9) because more H_2O_2 is electrogenerated by the ACF cathode [30]. Comparision of no current and 0.12 A of Fig. 7 allows the conclusion that mineralization is obviously enhanced in the presence of electrogeneration of H_2O_2, since in this case, the

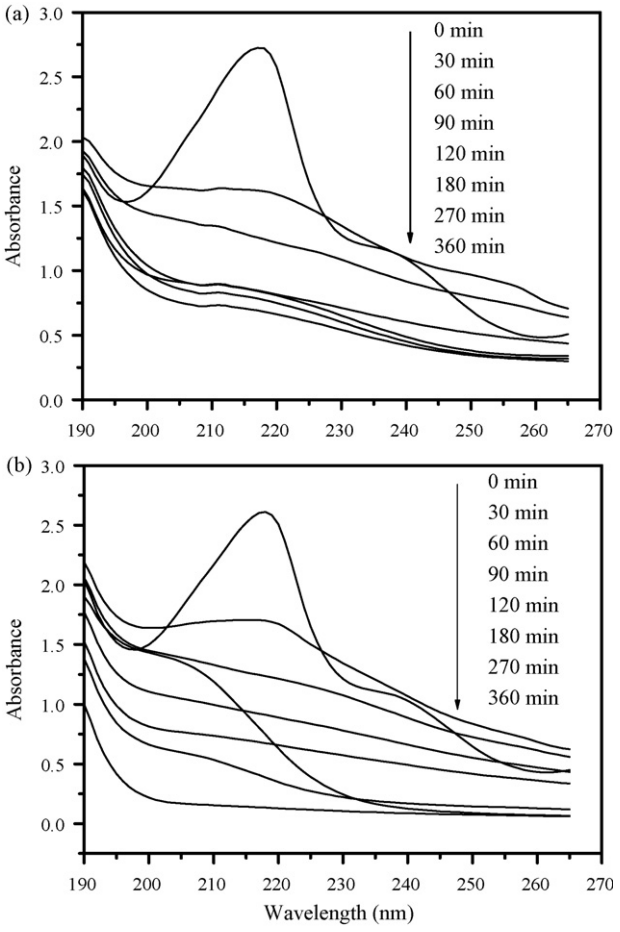

Fig. 6. Comparitive UV/vis spectral changes in the range of 190–265 nm with electrolysis time for 450 mL of 200 mg l^{-1} AR14 solution in 0.05 M Na_2SO_4 of pH 3.0 during (a) electro-Fenton and (b) photo-Fenton process. Applied current = 0.36 A.

solution TOC is reduced by only 15% after 6 h of simple UV oxidation, instead of more than 94% TOC removal for 0.12 A–0.50 A after 6 h PEF process. This behavior can be accounted for large amount H_2O_2 generated by ACF cathode, which can enhance the reaction of pollutants with •OH generated from Fenton reaction and H_2O_2 photolysis. However, it is obvious that when the current density is 0.50 A, the mineralization decreases. This is indicative of a slower relative generation of oxidant •OH due to the fact that when the current density is much high, H_2O_2 might be anodically oxidized to yield intermediate $HO_2^•$ radicals (Eqs. (12) and (13)), which is a less powerful agent than •OH.

$$H_2O_2 \rightarrow HO_2^• + H^+ + e^- \quad (12)$$

$$HO_2^• \rightarrow O_2 + H^+ + e^- \quad (13)$$

3.5. Effect of the type of iron ion

Several experiments were further performed to clarify the effect of Fe^{2+} and Fe^{3+} on the photoelectro-Fenton process, while the effect on the EF process was also investigated. As shown in Fig. 8, the type of iron ion has very little influence on the PEF and EF process, although the mineralization was a bit faster than that of Fe^{3+}catalyst when Fe^{2+} was used as catalyst for both processes. These results are indicative of the fast regeneration of Fe^{3+} at its surface when ACF felt was used for cathode in both processes, as explained by Sires et al. [22], who had testified that the Fe^{2+} could be electrogenerated very fast at a carbon-felt cathode in electro-Fenton process by the reaction (3).

The Fe^{2+} was also continuously regenerated in small extent for the reaction of Fe^{3+} in the medium with electrogenerated H_2O_2 by reaction (14) with $k_2 = 3.1 \times 10^{-3}\ M^{-1}\ s^{-1}$, with hydroperoxyl radical by reaction (15) with $k_2 < 1 \times 10^{-3}\ M^{-1}\ s^{-1}$, and/or with organic radical intermediates R• by reaction (16) [19,21]. Moreover, in PEF process, the electrogeneration of Fe^{2+} could also be enhanced by reaction (5) and (6), so the type of iron ion has little influence on the EF and PEF reaction for degradation of AR14.

$$Fe^{3+} + H_2O_2 \rightarrow Fe^{2+} + H^+ + HO_2^• \quad (14)$$

$$Fe^{3+} + HO_2^• \rightarrow Fe^{2+} + H^+ + O_2 \quad (15)$$

$$Fe^{3+} + R^• \rightarrow Fe^{2+} + R^+ \quad (16)$$

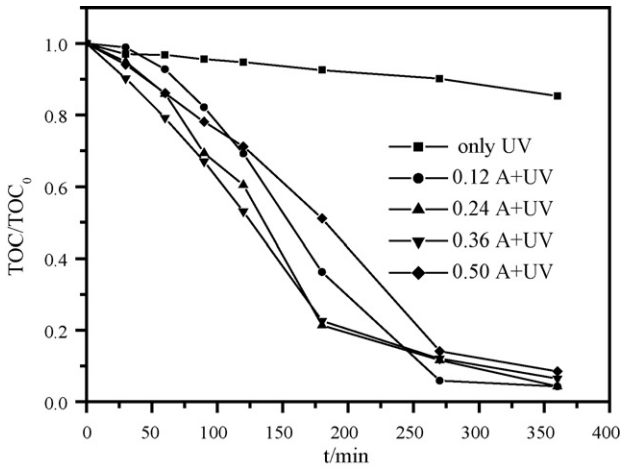

Fig. 7. Effect of current density on TOC removal decay during the photoelectro-Fenton treatment of 450 mL of 200 mg L^{-1} AR14 solutions in 0.05 M Na_2SO_4 of pH 3.0 using ACF cathode.

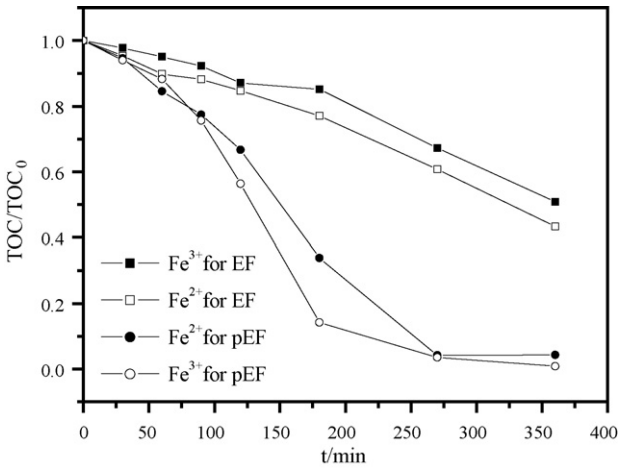

Fig. 8. Effect of iron ion type on TOC removal decay during the photoelectro-Fenton treatment of 450 mL of 200 mg L^{-1} AR14 solutions in 0.05 M Na_2SO_4 of pH 3.0 at 0.36 A using ACF cathode. Fe^{2+}: 1 mM, Fe^{3+}: 1 mM.

3.6. Effect of initial AR14 concentration

The oxidation ability of the PEF system with 1 mM Fe^{2+} to degrade AR14 concentrations $\leq$0.5 g L^{-1} of pH 3.0 at 0.36 A was also examined. A series of trials for different concentration AR14 solutions were carried out to test the influence of initial pollutant concentration on the PEF process, as well as to compare the MCE of different initial AR14 concentration in the PEF process.

Fig. 9a shows that almost total mineralization is attained for up to 300 mg L^{-1} of AR14 within 360 min electrolysis, whereas 16% and 21% TOC remain in solution for 400 and 500 mg L^{-1} AR14 solutions, respectively, and alter prolonged electrolysis, these solutions can be mineralized up to 95% (7 h for 400 mg L^{-1} AR14)–98% (8 h for 500 mg L^{-1} AR14). Fig. 9b presents the MCE-time plots for the experiments of Fig. 9a. As can be seen, the efficiency increases with rising AR14 concentration, indicating a faster removal of larger amounts of organics. Because the same production of •OH is expected from reaction (2), (6), (8) and (9) in all trials, it seems plausible to consider that its competitive nonoxidizing reactions become slower and more •OH concentration can than react with pollutants [20]. The MCE progressively rises during longer times at early stages of the treatment, reaching a maximum value of 38% for 500 mg L^{-1} at 2 h. This suggests an increasing formation of products that react more easily with •OH than the AR14 at early stages of electrolysis.

3.7. Effect of initial pH

To investigate the influence of pH on photoelectro-Fenton process, a series of experiments are carried out at various initial pH levels of 1.49, 2.04, 3.03, 3.97, 4.98, 6.04 and 6.72. Many studies have revealed that the solution pH can dramatically influence the Fenton degradation of organic compounds and at higher rates in the region 2.5–4, with an optimum at pH 3 [39]. At too high pH, the decomposition rate decreases because of the decrease of the free iron species in the solution, due to the formation of Fe(II) complexes and the precipitation of ferric oxyhydroxides [40]. When the pH is too low and the concentration of hydrogen ions is too high, it will slow down the formation of $FeOOH^{2+}$, which consecutively causes the production rates of ferrous ions and hydroxyl radicals to decrease as well [41].

Fig. 10 displays the TOC removal when initial solution pH is varied. Clearly, the degradation of AR14 is not significantly

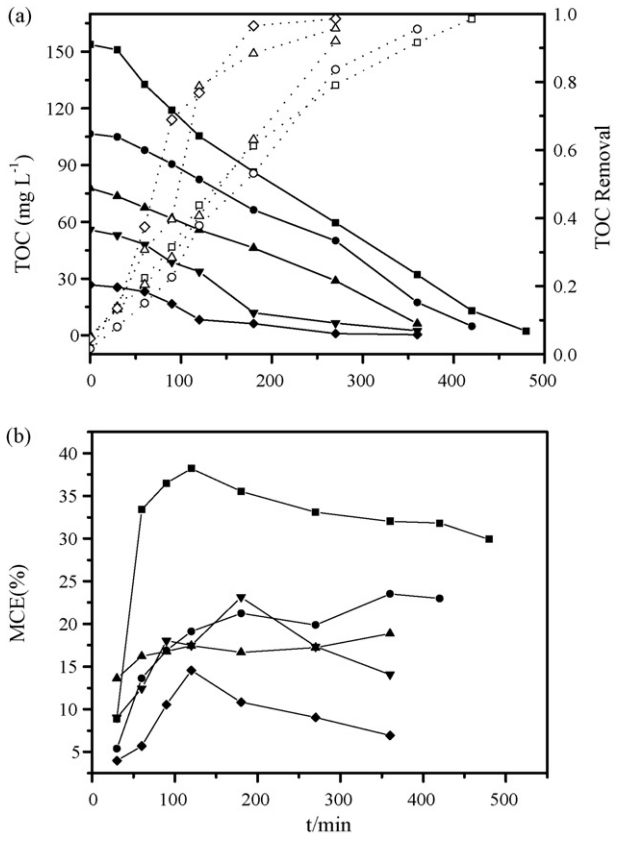

Fig. 9. (a) TOC abatement with electrolysis time for the photoelectro-Fenton degradation of 450 mL solutions of pH 3.0 containing AR14 concentrations of (■, □) 500, (●, ○) 400, (▲, △) 300, (▽, ▼) 200, and (◆, ◇) 100 mg L^{-1} using 1 mM Fe^{2+} at 0.36 A. (b) Change of the mineralization current efficiency calculated from Eq. (6) with time for the same experiments.

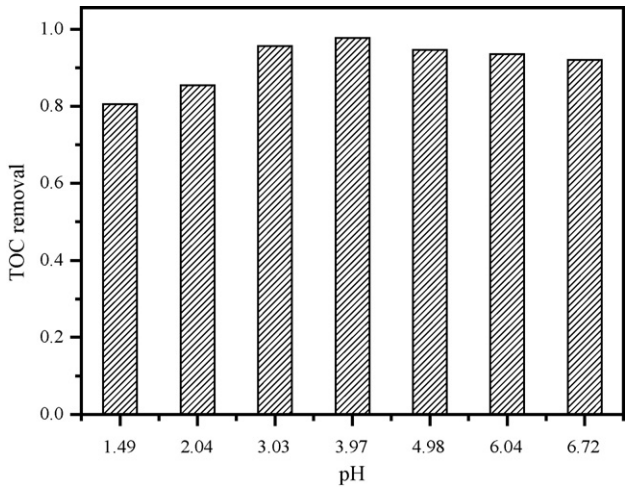

Fig. 10. TOC removal versus different initial pH for photoelectro-Fenton degradation of 450 mL of 200 mg L^{-1} AR14 solutions in 0.05 M Na_2SO_4 at 0.36 A using ACF felt cathode and RuO_2/Ti anode.

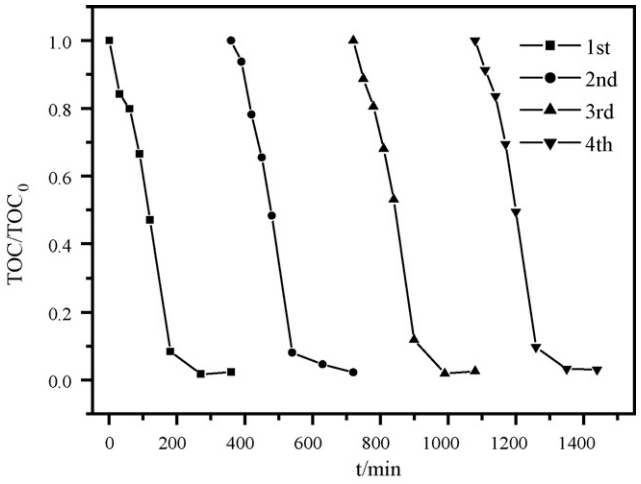

Fig. 11. TOC removal as a function of the reaction time up to four runs during photoelectro-Fenton process. AR14 concentration = 200 mg L^{-1}; pH 3.0; Fe^{2+} concentration = 1 mM; current density = 0.36 A.

influenced by the solution pH, which is similar to the results observed in the heterogeneous photoassisted Fenton reaction, and the high efficiency of photoelectro-Fenton was observed at a pH 3.97 in the region about 3.03–4.98, which is much wider than the optimal pH range for Fenton reaction. This is attributed to the pH change during photoelectro-Fenton degradation process. The final pH values after 6 h of electrolysis were 2.03 for an initial pH of 2.04, 2.85 for an initial pH of 3.05, 3.02 for an initial pH of 3.97, 3.00 for an initial pH of 4.90, 3.04 for an initial pH of 6.04, and 3.21 for an initial pH of 6.72. The change in the solution pH is related to the acidity of the intermediates produced during the degradation of AR14. A similar phenomenon was reported by Feng et al. [42] and Dhananjeyan et al. [43] in photoassisted Fenton degradation of azo dye Orange II mediated by heterogeneous Fenton reaction. They attributed the drop in the solution pH to two main factors. One is that mineralization of AR14 produces H^+ as shown in Eq. (10), which can contribute to acidify the solution. The other is that the intermediate Fe complexes consisting of Fe chelates are formed, leading to carboxylic acids during the degradation of AR14, such as oxalic, formic, and acetic acid, and smaller concentrations of other acids.

3.8. Long-term stability of photoelectro-Fenton process

A study on the stability of the catalytic activity of PEF process for the degradation of AR14 was conducted through multiple runs using identical reaction conditions. Fig. 11 presents the repetitive AR14 degradation in 6 h cycles under photoelectro-Fenton process using the same ACF cathode. At the end of each degradation cycle, 450 mL 200 mg L^{-1} ARB solution at pH 3.0 containing 1 mM Fe^{2+} was added to the reactor. Clearly, no obvious deactivation of the PEF process in successive cycles was observed when compared with the first cycle, which indicates that the PEF process has an excellent long-term stability. The excellent stability of the catalytic activity could be attributed to the stable structure of ACF cathode, which can electrogenerate enough H_2O_2 for photoelectro-Fenton reaction.

4. Conclusions

Acidic aqueous solutions with 200 mg L^{-1} of AR14 are completely degraded using photoelectro-Fenton process with an ACF cathode and Fe^{2+} as catalyst. Exhaustive mineralization of AR14 in acid aqueous media could be achieved by this process. Compared with the poor mineralization by anodic oxidation UV irradiation yields and electro-Fenton, photoelectro-Fenton allows a more effective mineralization of AR14 solutions, even at low current density, by the action of UV irradiation. An increase in

current density causes a faster mineralization in PEF process, while the mineralization current efficiency of PEF process was much higher than that in EF process and increases with rising AR14 concentration. The initial solution pH range 1.49–6.72 has little influence on the TOC removal because of the pH change during AR14 degradation in the PEF process, which may be due to the formation of organic carboxylic acids such as oxalic acid. The PEF process using ACF cathode is also used in multiple runs for the degradation of AR14, total mineralization all can be reached for four runs, which confirms its long-term stability and indicates its potential application for the removal of refractory organic pollutant in the water.

Acknowledgements

The authors gratefully acknowledge the financial support of this work by the National Natural Science Foundation of China (No. 50608068) and National Science Fund for Distinguished Young Scholars (No. 50225824).

Reference

[1] A.B. Prevot, C. Baiocchi, M. Brussino, E. Pramauro, P. Savarino, V. Augugliaro, G. Marci, L. Palmisano, Environ. Sci. Technol. 35 (2001) 971–976.
[2] C. Flox, S. Ammar, C. Arias, E. Brillas, A.V. Vargas-Zavala, R. Abdelhedi, Appl. Catal. B 67 (2006) 93–104.
[3] J.S. Do, C.P. Chen, Ind. Eng. Chem. Res. 33 (1994) 387–394.
[4] J.S. Do, W.C. Yeh, J. Appl. Electrochem. 28 (1998) 703–710.
[5] M. Panizza, G. Cerisola, Water Res. 35 (2001) 3987–3992.
[6] C. Ponce de Leon, D. Pletcher, J. Appl. Electrochem. 25 (1995) 307–314.
[7] A. Alvarez-Gallegos, D. Pletcher, Electrochim. Acta 44 (1998) 853–861.
[8] A. Alvarez-Gallegos, D. Pletcher, Electrochim. Acta 44 (1999) 2483–2492.
[9] Y.L. Hsiao, K. Nobe, J. Appl. Electrochem. 23 (1993) 943–946.
[10] T. Tzedakis, A. Savall, M.J. Clifton, J. Appl. Electrochem. 19 (1989) 911–921.
[11] M.A. Oturan, J.J. Aaron, N. Oturan, J. Pinson, Pestic. Sci. 55 (1999) 558–562.
[12] M.A. Oturan, J. Pinson, J. Electroanal. Chem. 334 (1992) 103–109.
[13] M.A. Oturan, J. Pinson, N. Oturan, D. Deprez, New J. Chem. 23 (1999) 793–794.
[14] M.A. Oturan, J. Appl. Electrochem. 30 (2000) 475–482.
[15] B. Gozmen, M.A. Oturan, N. Oturan, O. Erbatur, Environ. Sci. Technol. 37 (2003) 3716–3723.
[16] M.A. Oturan, N. Oturan, C. Lahitte, S. Trevin, J. Electroanal. Chem. 507 (2001) 96–102.
[17] M.A. Oturan, J. Peiroten, P. Chartrin, A.J. Acher, Environ. Sci. Technol. 34 (2000) 3474–3479.
[18] M.A. Oturan, J. Pinson, J. Phys. Chem. 99 (1995) 13948–13954.
[19] E. Brillas, P.L. Cabot, F. Centellas, J.A. Garrido, R.M. Rodriguez, Portug. Electrochim. Acta 24 (2006) 159–189.
[20] I. Sires, J.A. Garrido, R.M. Rodriguez, P.L. Cabot, F. Centellas, C. Arias, E. Brillas, J. Electrochem. Soc. 153 (2006) D1–D9.
[21] J. Casado, J. Fornaguera, M.I. Galan, Environ. Sci. Technol. 39 (2005) 1843–1847.
[22] I. Sires, J.A. Garrido, R.M.C. Rodriguez, E. Brillas, N. Oturan, M.A. Oturan, Appl. Catal. B 72 (2007) 382–394.
[23] B. Boye, M.M. Dieng, E. Brillas, J. Electroanal. Chem. 557 (2003) 135–146.
[24] E. Brillas, E. Mur, R. Sauleda, L. Sanchez, J. Peral, X. Domenech, J. Casado, Appl. Catal. B 16 (1998) 31–42.
[25] E. Brillas, J. Casado, Chemosphere 47 (2002) 241–248.
[26] E. Brillas, B. Boye, M.A. Banos, J.C. Calpe, J.A. Garrido, Chemophere 51 (2003) 227–235.
[27] B. Boye, M.M. Dieng, E. Brillas, Environ. Sci. Technol. 36 (2002) 3030–3035.
[28] C. Flox, J.A. Garrido, R.M. Rodríguez, P.L. Cabot, F. Centellas, E. Brillas, Catal. Today 129 (2007) 29–36.
[29] C. Flox, P.L. Cabot, F. Centellas, J.A. Garrido, R.M. Rodríguez, C. Arias, E. Brillas, Appl. Catal. B 75 (2007) 17–28.
[30] A.M. Wang, J.H. Qu, J. Ru, H.J. Liu, J.T. Ge, Dyes Pigments 65 (2005) 227–233.
[31] J.D. Rodger, N.J. Bunce, Environ. Sci. Technol. 35 (2001) 406–410.
[32] B.E. Conway, E. Ayranci, H. Al-Maznai, Electrochim. Acta 47 (2001) 705–718.
[33] S. Irmak, H.I. Yavuz, O. Erbatur, Appl. Catal. B 63 (2006) 243–248.
[34] J.T. Ge, J.H. Qu, Appl. Catal. B 47 (2004) 133–140.
[35] R.A. Torres, C. Petrier, E. Combet, F. Moulet, C. Pulgrin, Environ. Sci. Technol. 41 (2007) 297–302.
[36] F. Wu, N.S. Deng, H.L. Hua, Chemosphere 41 (2000) 1233–1238.
[37] Y. Xiong, P.J. Strunk, H.Y. Xia, X.H. Zhu, H.T. Karlsson, Water Res. 35 (2001) 4226–4230.
[38] M. Stylidi, D.I. Kondarides, X.E. Verykios, Appl. Catal. B 40 (2003) 271–286.
[39] A.A. Burbanoa, D.D. Dionysioua, M.T. Suidana, T.L. Richardson, Water Res. 39 (2005) 107–118.
[40] F.J. Benitez, J.L. Acero, F.J. Real, F.J. Rubio, A.I. Leal, Water Res. 35 (2001) 1338–1343.
[41] E. Neyens, J. Baeyens, J. Hazard. Mater. B 98 (2003) 33–50.
[42] J.Y. Feng, X.J. Hu, P.L. Yue, H.Y. Zhu, G.Q. Lu, Ind. Eng. Chem. Res. 42 (2003) 2058–2066.
[43] M.R. Dhananjeyan, J. Kiwi, P. Albers, O. Enea, Helv. Chim. Acta 84 (2001) 3433–4344.